RSC Advances

PAPER

View Article Online
View Journal | View Issue



Cite this: *RSC Adv.*, 2021, **11**, 3963

# Pickering-emulsion-templated synthesis of 3D hollow graphene as an efficient oil absorbent†

Nurul Aqilah Pohan, [a] Mohd Haniff Wahid, *[a] Zulkarnain Zainal [ab] and Nor Azowa Ibrahim[a]

The preparation of graphene in three-dimensional mode represents an alternative method to maintain its characteristically large surface area, which, under normal circumstances, is diminished by the restacking of the individual sheets. Sufficiently stable 3D graphene enables the high surface area characteristic of monoatomic graphene layers to be obtained. Based on the coupling of the high surface area and the void spaces that are thus created, which act as pores, 3D graphene is anticipated to have potential as a sorbent material. In this study, lightweight 3D hollow graphene featuring a unique thin skeletal framework was developed using the Pickering emulsion route for oil absorbent applications. In this technique, toluene droplets stabilized by graphene oxide layers in a water system were used as the template, and upon the removal of the solvent by freeze-drying and microwave-assisted reduction, 3D hollow graphene was obtained. The produced 3D graphene demonstrates excellent sorption efficiencies of 84 to 145 g $g^{-1}$ for different types of oil and organic solvents in the first absorption. This excellence can be attributed to its multi-level porosity as elucidated by mercury intrusion porosimetry (MIP) and Brunauer–Emmett–Teller (BET) surface area analysis, which indicated a bimodal pore size distribution with macroporosity and mesoporosity and a surface area of 127 $m^2$ $g^{-1}$. The 3D hollow graphene prepared using the Pickering emulsion template technique incorporating microwave treatment can be readily recycled using a solvent extraction process for a total of ten sorption–desorption cycles without significant losses in its efficiency, making it promising for further consideration as an appropriate material for oil spill incidents.

Received 30th October 2020
Accepted 16th December 2020

DOI: 10.1039/d0ra09265g

rsc.li/rsc-advances



## Introduction

Over the past two decades, the total global output of crude oil has risen from about 3.5 billion metric tons in 1998 to about 4.5 billion metric tons in 2019.[1] The huge increase in this commodity is mainly due to the oil dependence of the world economy. In cases where the pipeline infrastructure for oil transportation is limited, large volumes of oil must be transported by land or sea. In 2018 alone, over two billion metric tons of crude oil were transported *via* waterways.[1] However, the rapid growth of oil transportation activities *via* seaway lanes increases the risk of oil spillage in sea areas. For example, very recently, a total of nearly 4000 tons of diesel and oil was spilled in the Indian Ocean off Mauritius Island, placing the country in a state of environmental emergency.[2] As the country struggled with their first oil spill incident, the devastating impact of such occurrences in the past has taught us that an immediate and effective clean-up is vital to prevent the coverage of a large water surface area by the spilled oil, which may cause ecological alterations and the prolonged elimination of rare species. Various methods are used for oil spill remediation, including mechanical collection and *in situ* burning; however, the gaseous chemicals generated by combustion pollute the atmosphere. Likewise, the deployment of oil containment booms can confine the oil in a particular collection spot, but turbulent surfaces and wave conditions limit their practicality.[3] Therefore, the employment of absorbents is promising as a potential strategy to overcome these drawbacks, as they offer several advantages including low production cost and easy fabrication.[3]

Graphene, which is composed of a single atomic layer of $sp^2$ hybridized carbon atoms, is a disruptive material used in various applications, such as energy storage,[4] electronic devices,[5] gas storage,[6] sensors,[7] catalysis[8] and water security.[9] It is also a promising material for sorption applications due to its high theoretical surface area (2630 $m^2$ $g^{-1}$), chemical stability and mechanical strength.[10] However, the isolation of monoatomic layers of graphene is inherently challenging, as these single layers are thermodynamically unstable. Van der Waals interactions drive the tendency of the layers to restack onto one another, diminishing their surface area.[11] Therefore, the

[a]*Department of Chemistry, Faculty of Science, Universiti Putra Malaysia, 43400 Serdang, Selangor, Malaysia. E-mail: mw_haniff@upm.edu.my*

[b]*Material Synthesis Laboratory, Institute of Advanced Technology, Universiti Putra Malaysia, 43400 Serdang, Selangor, Malaysia*

† Electronic supplementary information (ESI) available. See DOI: 10.1039/d0ra09265g

development of graphene with a 3D configuration represents an alternative path to preserving the high surface area characteristic of this material.[12] Furthermore, the construction of 3D graphene paves the way for the development of an interconnected porous network within the graphene structure. It has been reported that microporosity and mesoporosity imbue such materials with a high surface area, while accessibility to their sorption sites is determined by their hydrophobicity and macroporosity.[13]

Several methods have been reported for the construction of 3D graphene, such as carbonisation of a polymer framework,[14] freeze-drying,[15] sugar-blowing,[16] cross-linking assembly[17] and the Pickering emulsion technique.[18] Given its advantages in terms of cost, quality and sustainability, the demand for applications based on the Pickering emulsion technique has begun to increase in various industries.[19] This method offers sustainability, as unlike conventional template-based synthesis, it does not require the use of hard templates, and it is also scalable.[18] Furthermore, since toluene droplets are used as the template, this method provides a greater chance to control the microstructure of the 3D graphene through the manipulation of the liquid interfaces.[18,19]

Prior studies have demonstrated the use of graphene-based materials in holistic approaches to water security applications. For example, Kamaraj *et al.* (2017) reported the adsorption of chlorophenoxyacetic acid herbicides using graphene nanosheets, achieving 70–86% removal.[20] Additionally, Ganesan *et al.* (2013) reported the adsorption of $NO_3^-$ with an initial concentration of 500 mg $L^{-1}$ using graphene, culminating in 89.97 mg $g^{-1}$ removal, while Vasudevan *et al.* (2012) reported phosphate adsorption at 303 K with 89.37 mg $g^{-1}$ removal.[21,22] The wide range of sorption abilities exhibited by graphene-based materials was further extended by the work of Tabish *et al.* (2018), who described the synthesis of thermally treated porous reduced graphene oxide for the adsorption of oils and organic dyes.[23] The graphene aerogel synthesized by Cheng *et al.* (2017) showed 99.7% porosity and the capacity to absorb various oils and organic solvents within 20 seconds.[24] Likewise, the spongy graphene prepared by Bi *et al.* (2014) showed an excellent sorption ability of 616 times its own weight for various oils and organic solvents, particularly chloroform.[25] Song *et al.* (2016) used an ultrasonic microwave-assisted synthesis to prepare reduced-graphene-oxide-modified melamine foam that could absorb oils and organic solvents and could be reused up to 20 times.[26]

In this study, lightweight 3D hollow graphene featuring a thin skeletal framework was fabricated *via* three steps. First, a Pickering emulsion of graphene-oxide-stabilized toluene droplets in water was prepared and subsequently subjected to bath sonication for two hours (Fig. 1a–c). The second step involved the removal of the solvent using the freeze-drying technique, which yielded a light and fluffy 3D hollow graphene material (inset image in Fig. 1d). Since hydrophobicity was a requirement for oil absorption in this study, a third step was introduced, in which the graphene oxide was reduced to restore the $sp^2$ hybridization of the graphene. This process was carried out using a microwave-assisted reduction technique. It

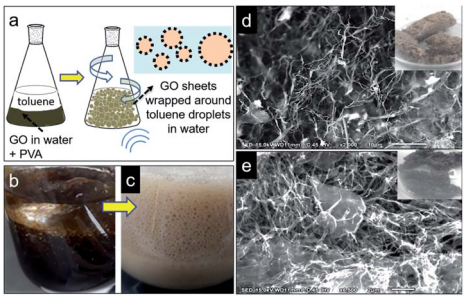


Fig. 1 Synthesis of 3D hollow graphene. (a) Schematic illustration of 3D hollow graphene preparation. (b) Photograph of the distinct layers observed upon mixing toluene with graphene oxide and PVA in water. (c) Homogeneous brown emulsion obtained after gentle swirling and bath sonication. (d) SEM image of the 3D hollow graphene supported by a thin skeletal framework (inset: photograph of the 3D hollow graphene after freeze-drying). (e) SEM image of the 3D hollow graphene after reduction, showing that the 3D porous structure is retained (inset: photograph image of the 3D hollow graphene after exposure to microwave irradiation; the sample colour changed from light-brown to black).

is worth mentioning that the development of 3D hollow graphene from 2D graphene using a Pickering emulsion technique has been reported previously.[18] However, the as-prepared 3D hollow graphene in this work provided abundant porous channels, a high accessible surface area and an outstanding selective uptake of oil in the seawater paradigm. The sorption capacity of the reduced 3D hollow graphene towards different types of oil and organic solvents was investigated and compared with those of a commercial analogue and other 3D graphene-based materials from the literature. The regeneration of the reduced 3D hollow graphene was examined over ten cycles of oil uptake to enhance its practicality and provide economic insight. Furthermore, parameters such as the presence of polyvinyl alcohol (PVA), bath sonication and microwave temperature were studied to examine their effects on the morphology of the 3D hollow graphene and its textural properties with the aim of producing a highly porous framework, which would make the material not only an ideal candidate for water treatment, but also a potentially viable alternative for other applications such as energy storage, photocatalysis, and enzyme modulation.

## Results and discussion

### Physicochemical characterization of 3D hollow graphene

The morphology of the obtained 3D hollow graphene was investigated using scanning electron microscopy (SEM), and the results are shown in Fig. 1d and e. The graphene sheets are randomly oriented and interconnected with PVA chains to form a 3D structure with various pore sizes and shapes. The SEM images also demonstrate that the structure is supported by a distinct thin layered material acting as the framework, which most likely consists of layers of graphene/PVA composite. The high porosity and thin framework of the 3D hollow graphene make it an ideal absorbent material. After the reduction of graphene oxide using the microwave irradiation technique, the

3D porous structure is retained, as shown in Fig. 1d. Sengupta *et al.* reported that GO absorbs microwave energy due to the functional oxygen groups associated with the composition of moisture-molecules, causing it to vibrate at an impressive rate of *ca.* 2 450 000 000 times per second, thus triggering thermal shock. Microwave irradiation induces reduction by creating sufficient thermal shock to eliminate the oxygen functionalities from the carbon plane of GO lattice in the form of water vapour, CO and $CO_2$. In addition, the gas evolution creates pressure between stacked layers of GO, thus promoting exfoliation and volume expansion.[27]

In comparison to the material described in the previous work of Chen *et al.* (2014), the sample obtained in this study displays a unique interconnected thin skeletal framework and is more porous.[18] The role of PVA in the construction of the 3D structure is important, as the PVA chains interact with the graphene oxide sheets, acting as a reinforcement material to maintain the 3D structure after solvent removal by freeze-drying.[17] The abundant voids and pores resulting from 3D graphene construction are desirable for the whole state absorption of molecules.[28] Absorption performance is closely related to the presence of macropores, which is demonstrated in Fig. 1, in which pores with diameters greater than 10 μm are observed. This size is sufficiently high to decrease pore blockage by oils and organic solvent molecules during the absorption process. In addition, the presence of macropores allows increased diffusion in the porous channels, resulting in greater absorption ability.[13,28] Tao (2014) reported that the presence of mesopores as side branches of larger pores facilitates oil retention in the pore network.[29] Additionally, mesopores introduce roughness on the surface of the macropores, enabling dispersive interactions between carbon basal planes and adsorbate molecules.[29]

Brunauer–Emmett–Teller (BET) surface area and porosity analysis of the samples was conducted, and mercury intrusion porosimetry (MIP) was carried out to complement the BET analyses. The nitrogen gas adsorption isotherm and Barrett–Joyner–Halenda (BJH) pore size distribution curves of the 3D hollow graphene (3D GO) and reduced 3D hollow graphene (3D r-GO) are depicted in Fig. 2, and the results are summarized in Table 1. BET analysis shows that the gas adsorption isotherm obtained for the 3D GO samples is of type IV. The presence of a hysteresis loop and the results of the pore size distribution analysis indicate that the sample is mesoporous (Fig. 2). Nevertheless, it is noteworthy to point out that in cases in which a mesoporous sample contains no macropores, its isotherm will remain nearly horizontal at the upper range of $p/p^0$, indicative of equilibrium. However, the isotherms of the samples obtained in this study displayed an increasing trend even at $p/p^0 = 1$, thus indicating the presence of macropores.[30] Given the presence of multilevel meso- to macroporosity, MIP analysis was used to complement the BET analysis. As shown in Fig. ESI S2,† the presence of a large amount of macropores with diameters above 50 nm and of mesopores of 3–5 nm was detected. The surface area analysis revealed an improvement in the BET surface area from 36 $m^2\ g^{-1}$ for the graphene oxide precursor to 104 $m^2\ g^{-1}$ for the 3D GO. This demonstrates the suitability of the approach in preserving the surface area of graphene. Furthermore, our

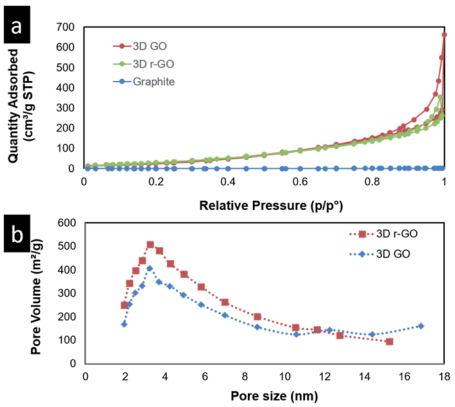


Fig. 2 Surface area analysis of graphite, 3D GO and 3D r-GO. (a) Nitrogen adsorption–desorption isotherms measured at 78 K, showing the type IV isotherms of the 3D GO and 3D r-GO samples. Note that the samples did not achieve equilibrium at the upper range of p/p°, indicating that they contain macropores. (b) Barrett–Joyner–Halenda pore size distribution curves.

samples showed slight improvements in their surface area values compared to those in previous studies;[18,28] the porosity values of the obtained 3D structures ranged from 89 to 95%, which are among the highest reported.[31] Despite the surface area increase, it is firmly assumed that with the existence of large numbers of macropores, the diffusion of oil into the large macro-channels in the bulk material will be greatly enhanced, as is evident from the results of the MIP analysis (Fig. S2†).

Hydrophobicity drives the segregation of water-insoluble molecules from an aqueous medium. It is the main mechanism for oil absorption from water, as it prevents the absorption of water molecules into pores and increases the selectivity towards hydrocarbon chains. Thus, by increasing the hydrophobicity of a sorbent, its efficiency in the sorption of oil from water will increase. Since the 3D GO has oxygen functional groups, which have a great affinity for water, it must be reduced to recover the hydrophobicity of graphene. In this study, the reduction process was performed using microwave irradiation.

Fourier-transform infrared spectroscopy (FTIR) was used to confirm the success of the functionalization steps from bulk graphite and continuing to the formation of 3D r-GO. The results are shown in Fig. 3. For pristine graphite, discernible peaks at 3000–3100 $cm^{-1}$, which correspond to aromatic C–H bonds, were replaced by broad absorption peaks after oxidation, which were attributed to the stretching of hydroxyl groups. Furthermore, upon the oxidation of graphite, emerging peaks at 1720 $cm^{-1}$ and 1200 $cm^{-1}$ were observed, corresponding to the absorption of carbonyl and epoxy functional groups, respectively. Meanwhile, the 3D GO spectra showed absorption peaks similar to those of GO, but with more clear and broader hydroxyl group peaks, suggesting the successful integration of PVA into the 3D GO structure. A decrease in the intensities of the peaks at 1720 $cm^{-1}$ and 1200 $cm^{-1}$ due to the absorption of carbonyl and epoxy functional groups was observed at the reduction stage. Additionally, a visible change in colour from light brown to black occurred, confirming the effective

Table 1 Summary of the surface area and porosity analysis of the 3D hollow graphene and reduced 3D hollow graphene

| Sample | BET surface area ($m^2\ g^{-1}$) | Pore volume ($mL\ g^{-1}$) | Pore diameter (nm) | Porosity (%) |
|---|---|---|---|---|
| GO | 36 | 0.14 | 5 | — |
| 3D GO | 104 | 0.35 | 5 | 95 |
| 3D r-GO | 127 | 0.28 | 5 | 89 |

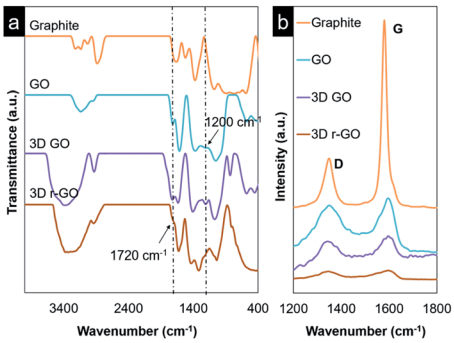


Fig. 3 (a) FT-IR spectra of graphite, graphene oxide, 3D hollow graphene and reduced 3D hollow graphene. The emergence of absorption peaks at 1720 $cm^{-1}$ and 1200 $cm^{-1}$ indicates the oxidation of graphite; upon reduction, the peaks disappear. (b) Raman spectra of graphite, graphene oxide, 3D hollow graphene and reduced 3D hollow graphene.

reduction of GO and anomalous restoration of the $sp^2$ hybridization of graphene through the removal of some oxygen functional groups. The binding energy of the hydroxyl groups attached to the inner part is lower than that of similar groups attached to the edge, so hydroxyl group peaks were still visible in the spectra after reduction,[27] since the critical dissociation temperature for hydroxyl groups at the edges is 650 °C. The reduction of carboxyl groups starts at 100–150 °C, but functional groups such as carbonyl and epoxy are removed as $CO_2$ and CO, causing disruption in the lattice and further promoting the exfoliation of the graphene sheets.[27]

The chemical changes in the graphene were further confirmed by Raman analysis. The signature D and G band peaks of graphene-based materials were observed in the 3D GO samples before and after the reduction of graphene oxide, indicating that the graphene structure was preserved throughout the entire process (Fig. 3b). The D band is associated with the size reduction of the in-plane $sp^2$ domain resulting from the oxidation of graphite. The degree of disorder in the $sp^2$ and $sp^3$ is reflected through the ratio $I_D/I_G$. The 3D GO displays a slightly higher degree of disorder, possibly due to the edge defects introduced in the sonication step prior to the formation of the 3D structure.[32] The 3D r-GO shows a lower $I_D/I_G$ value compared to that of 3D GO, suggesting the restoration of the $sp^2$ hybridization of graphene through the removal of some oxygen functional groups *via* microwave irradiation as mentioned earlier. In summary, both FTIR and Raman analyses complemented one another and attested to the successful formation of 3D r-GO.

Control experiments using different preparation conditions were carried out to investigate the effects of the PVA, sonication and microwave irradiation steps on the morphology and other surface characteristics. The SEM micrograph of 3D GO prepared without PVA exhibits the typical 2D features of graphene, with void spaces within the sheets. However, in the absence of PVA, the final product appears to be more compact and is fragile (inset image of Fig. 4a). This coincides well with the fact that PVA acts as a reinforcement additive to support the porous 3D structure.[17] Additionally, the preparation of 3D GO without sonication resulted in agglomeration in some parts of the sample (Fig. 4b) with higher pore volumes. In addition, the gas adsorption–desorption isotherm exhibits smaller hysteresis loops, indicating the different surface characteristics of the sample obtained (Fig. ESI S3†). Increasing the microwave irradiation temperature from 120 °C to 170 °C resulted in a higher surface area and pore volume, as shown in Table 2. However, the formation of the end-product was accompanied with a strong burnt smell. This might be due to overheating in the matrix, thus leading to burning of the sample in the presence of air, even though the thermal degradation temperature of PVA was ~200 °C based on TGA results (Fig. ESI S4†).[33] The increase in surface area and pore volume might be due to the thermal exfoliation of the graphene sheets and decomposition of PVA, respectively.

## Sorption capacity of the 3D hollow graphene

The 3D r-GO was used as a sorbent material after being subjected to microwave irradiation at 150 °C. Sorption studies using different types of used oil and organic solvents were carried out using a method similar to that of Riaz *et al.* (2017);

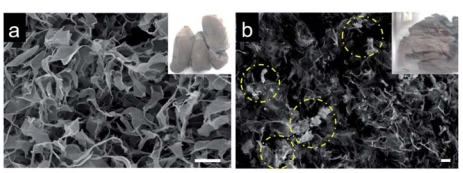


Fig. 4 Synthesis of 3D hollow graphene under different preparation conditions: (a) SEM image of the 3D hollow graphene prepared in the absence of PVA shows a ribbon-like structure instead of interconnected framework. (b) SEM image of the 3D hollow graphene prepared without sonication shows an interconnected 3D structure, but agglomerations of graphene sheets in the 3D framework (circled in yellow) were observed (scale bar: 10 μm).

Table 2 Summary of the surface area and porosity analysis of 3D hollow graphene obtained using different preparation conditions

| Sample | BET surface area ($m^2\ g^{-1}$) | Pore volume ($mL\ g^{-1}$) | Pore diameter (nm) |
|---|---|---|---|
| 3D GO (without PVA) | 99 | 0.40 | 5 |
| 3D GO (without sonication) | 121 | 0.43 | 5 |
| 3D r-GO (heated at 120 °C) | 48 | 0.14 | 5 |
| 3D r-GO (heated at 150 °C) | 133 | 0.39 | 5 |
| 3D r-GO (heated at 170 °C) | 354 | 0.95 | 5 |

50 mg of the absorbent was encased in a teabag, and two minutes of absorbent–absorbate contact time and a one-minute drainage period were employed (Fig. ESI S5†). The drainage time of one minute is required to ensure the proper removal of oil and solvent molecules loosely attached to the outermost teabag surface by cohesive and adhesive forces. Table 3 lists the excellent absorbencies of the 3D r-GO, which ranged from 131 to 145 g $g^{-1}$ for the oils and 84 to 114 g $g^{-1}$ for organic solvents. Several prior studies[34–36] have reported similar or greater sorption capacities; however, in these, the 3D r-GO was synthesized using different routes, rather than by the incorporation of microwave reduction with Pickering-emulsion templating.

Several factors promoting the sorption in this work have been identified, such as π–π bonding, density, hydrophobic interactions, and multi-level porosity. These findings are consistent with those reported in previous studies on various sorbent materials, such as a nanocellulose aerogel,[37] a reduced graphene oxide film,[38] Fe/C nanocomposites,[39] carbon microbelt aerogels,[40] a carbon fibre aerogel made from raw cotton,[41] a carbon aerogel made from kapok wadding materials[42] and 3D nitrogen-doped graphene.[43]

A thorough overview of the synthesis and sorption capacity obtained in this study and those in previously reported 3D graphene-based sorbents, such as r-GO coated melamine foam,[26] 3D graphene aerogel,[28] silanized graphene aerogel,[31] porous rGO foam,[44] KH-570 modified graphene coated PU sponge[45] and graphene PU sponge prepared through solvothermal treatment, is provided in Table 4.[46] The sorption capacity of 3D r-GO is indeed comparable to those of materials with high sorption capacity, for example, porous graphene (54–165 g $g^{-1}$),[23] rGO foam (90–123 g $g^{-1}$),[34] graphene sponge (54–165 g $g^{-1}$)[35] and rGO coated polyurethane sponge (80–160 g $g^{-1}$).[36] Although the sorption capacity of 3D r-GO is lower than that of melamine sponge coated with striped polydimethylsiloxane (103–179 g $g^{-1}$)[47] and graphene-CNT aerogel (100–270 g $g^{-1}$),[48] the fabrication method for 3D r-GO is scalable and free from the use of hard templates. The 3D r-GO in this work represents an alternative for the advancement of porous materials and a promising sorbent for the removal of oils and organic solvents.

Table 3 Sorption capacity of reduced 3D hollow graphene for various types of oils and organic solvents

| Sorbate | Sorption capacity (g $g^{-1}$) |
|---|---|
| Toluene | 103–107 |
| Used engine oil | 138–145 |
| Used vegetable oil | 128–131 |
| Ethanol | 108–110 |
| Methanol | 112–114 |
| Acetone | 102–105 |
| Hexane | 82–84 |

The 3D r-GO oil absorption performance was compared to a commercial absorbent pad obtained from Malaysian Maritime Agency under similar experimental conditions, and the results are depicted in Fig. 5.

The sorption capacity of the 3D r-GO is remarkable compared to that of the commercial absorbent. The uptake capacity of the 3D r-GO ranges from 84 to 145 g $g^{-1}$, whereas the commercial absorbent pad exhibits sorption capacities in the range of 45–62 g $g^{-1}$.

### Recyclability of the 3D r-GO

Since the goal of this work was to build an affordable, effective and sustainable oil sorbent material, ten sorption–desorption cycles with used engine oil were conducted for reusability testing. Solvent extraction was carried out by *n*-hexane flushing to remove the absorbed oil and recover the 3D r-GO foam. The sorption power, however, was found to decrease from 145 g $g^{-1}$ in the first cycle to 56 g $g^{-1}$ (Fig. 6), suggesting that the structural integrity of the graphene/PVA composite was compromised (Fig. ESI S6†). This was demonstrated by the FTIR spectra (Fig. ESI S6a†) of the 3D r-GO after the absorption of oil, in which the broad peaks attributed to hydroxyl, epoxy and carbonyl groups were found to have been greatly reduced. The SEM image (Fig. ESI S6b†) of 3D r-GO shows the disintegration of the 3D network of graphene/PVA; a paper-like structure was observed instead of the interconnected framework.

## Experimental

### Chemicals

Graphite powder (<20 μm) was obtained from Sigma Aldrich (Missouri, USA). Sulphuric acid ($H_2SO_4$, 98%), phosphoric acid ($H_3PO_4$, 98%), potassium permanganate ($KMnO_4$, 99%), toluene ($C_7H_8$, 99%), polyvinyl alcohol ($(C_4H_7O)_n$, $M_w$ 89 000–98 000, 99+% hydrolyzed) and hydrogen peroxide ($H_2O_2$, 30%) were obtained from Chemiz (Malaysia). Hydrochloric acid (HCl, 36%) was purchased from Systerm (Malaysia). All chemicals are

Table 4 Summary of the synthesis and sorption capacity of previously reported 3D graphene-based materials

| Absorbent | Sorption Capacity ($g\ g^{-1}$) | Method | Reference |
|---|---|---|---|
| Porous graphene | 54–165 | Argon thermal treatment | 23 |
| r-GO melamine foam | 57–112 | Ultrasonic–microwave synergistic treatment | 26 |
| 3D graphene aerogel | 58–70 | Hydrothermal treatment and freeze-drying | 28 |
| Graphene aerogel | 34–112 | Silanization | 31 |
| Porous rGO foam | 26–37 | Autoclave leavening | 44 |
| rGO foam | 90–123 | Freeze-drying | 34 |
| Graphene sponge | 54–165 | Dip coating | 35 |
| rGO coated polyurethane sponge | 80–160 | Coating with GO followed by reduction with hydrazine | 36 |
| KH-570 modified graphene coated PU sponge | 39 | Dip coating | 45 |
| Graphene PU sponge | 25–44 | Solvothermal treatment | 46 |
| Melamine sponge coated with striped polydimethyl siloxane | 103–179 | Thio-ene click reaction | 47 |
| Graphene-CNT aerogel | 100–270 | Hydrothermal redox reaction and freeze-drying | 48 |

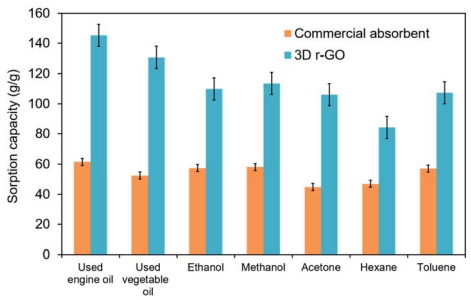


Fig. 5 Absorption efficiency comparison between the reduced 3D hollow graphene and a commercial absorbent pad for various kinds of oil and organic solvents.

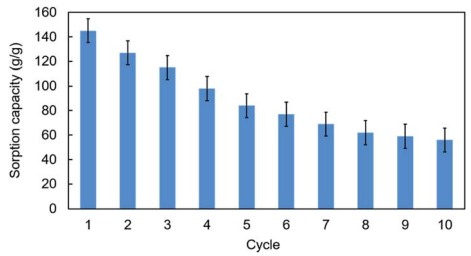


Fig. 6 Recyclability testing of the absorption of used engine oil on the reduced 3D hollow graphene using the solvent extraction method.

of analytical grade and were used as received without any further purification. The deionized (DI) water used for washing was obtained from a Milli-Q Plus system (Millipore). The used engine oil was obtained from a local motorcycle workshop in Sri Serdang, Malaysia.

## Material preparation

**Preparation of graphene oxide (GO).** Graphene oxide was prepared using a modified Hummers process.[49,50] Briefly, 3.0 g of pristine graphite was dispersed in a 9 : 1 acid mixture (400 mL) of concentrated $H_2SO_4/H_3PO_4$. Following this, 18.0 g of $KMnO_4$ was slowly added to the mixture and stirred for 72 hours. 35 mL of $H_2O_2$ was then added carefully to the mixture, which was stirred for 24 hours at room temperature to completely remove the excess $KMnO_4$ and terminate the oxidation process. Finally, before neutrality was attained, the graphite oxide was washed and centrifuged with 1 M HCl and excess DI water.

**Preparation of 3D GO.** The 3D hollow graphene was prepared using the method defined by Chen *et al.* (2014) with minor modifications.[18] In this study, a 1 wt% polyvinyl alcohol (PVA) solution (0.1 g PVA in 10 mL of DI water) was prepared, followed by the addition of 100 mL of 2 $mgmL^{-1}$ graphene oxide solution. The PVA/GO solution was subsequently mixed with toluene in a 1 : 1 volume ratio; the mixture was gently swirled to promote mixing of the immiscible solution.[51] The formation of two layers was observed, with a light-brown coloured foam at the top and a slightly darker-brown coloured solution at the bottom, indicating phase separation between the oil and water phases. The mixture was further treated by bath sonication for two hours to enhance the mixing and generate much smaller bubbles. The resulting emulsion was shaken vigorously before being frozen using liquid nitrogen to preserve the foam structure. The frozen mixture was freeze-dried for 64 hours.

**Preparation of 3D r-GO.** The reduction of the 3D hollow graphene oxide was conducted using a microwave irradiation technique (Fig. S1†) at 150 °C for 30 minutes with 15 minutes intervals using a conventional National Microwave oven; NN-C2000P, Japan.[27,52]

## Characterization

Surface functionalization was studied using a Perkin Elmer Spectrum 100 Fourier Transform Infrared (FTIR) spectrometer in the wavelength range of 4000–400 $cm^{-1}$. Raman measurements were carried out using a Witec Alpha 300R spectrometer (Germany) with a 532 nm laser under ambient temperature without any pretreatment. The Raman analysis was conducted to determine the presence of graphene material in the samples through the observation of the two intense peaks corresponding

to the D band (~1350 $cm^{-1}$) and G band (~1580 $cm^{-1}$). The background of the Raman spectra arises from the fluorescence property of graphene oxide.

The textural properties of the materials were analysed using the nitrogen gas adsorption–desorption method at 77 K with a Micromeritics Tristar II Plus Surface Analyzer (USA). To determine the surface area and pore size distribution, the Brunauer–Emmett–Teller (BET) and the Barrett–Joyner–Halenda (BJH) equations were used. Prior to analysis, the samples were outgassed at 120 °C to remove all the moisture and adsorbed gases on the products. Mercury intrusion porosimetry (MIP) was conducted to determine the porosity and macropore structure using a MicroActive AutoPore (Micromeritics, USA). The size of the pores was later compared with the definitions given by the International Union of Pure and Applied Chemistry (IUPAC).[30] Scanning electron microscopy (SEM) analysis was performed using a JEOL JSM-IT100 (Japan) to analyze the morphologies and surface characteristics of the samples. The samples were coated with gold using a Baltec SC030 Sputter Coater (Hi Tech, Germany) to eliminate charging effects and obtain clearer views of the micrograph.

### Sorption experiment

**Sorption capacity.** 50 mg of the 3D r-GO absorbent material was accurately weighed out, placed in a teabag casing, and reweighed. The absorbent was later submerged in beakers containing various oil and organic solvent sorbates, namely, toluene, methanol, ethanol, acetone, hexane, used engine oil, and used vegetable oil, for a contact time of 2 min to ensure complete absorption until the saturation limit was reached.[28] The samples were subsequently gently removed from the beaker and allowed to drain for one minute to remove weakly absorbed oil. Following this, the teabag containing the absorbent was immediately reweighed to determine the sorption capacity of the absorbent based on the amount of absorbate taken up per unit mass of dry absorbent, as shown in the eqn (1) below:

$$Q = [\,(W_i - W_f)/a] - c \quad (1)$$

where $Q$ is the sorption potential of the 3D graphene derivatives, and $W_i$ and $W_f$ are the initial and final weight of the absorbent in the teabag case. $a$ is the constant weight of absorbent used for all sorption experiments (50 mg), and $c$ is the constant average sorption capacity of the teabag alone, (7.95 g $g^{-1}$).

### Recyclability test

Reusability tests were conducted using a solvent extraction method using *n*-hexane (200 mL). The samples were placed in a rotary evaporator at 120 °C for 1 hour. The *n*-hexane dispersed into the 3D hollow graphene pores and flushed away the oil. The teabags containing the sample were later dried in an oven for 1 hour before being used in subsequent sorption cycles. The sorption capacities for each cycle were determined as previously mentioned in eqn (1).

## Conclusions

In conclusion, a porous lightweight 3D hollow nanostructured graphene framework was successfully fabricated, and its physicochemical properties were analysed. The absorbent possesses a unique microstructure featuring a thin skeletal framework of a graphene/PVA composite. Furthermore, the chemical reduction of GO *via* microwave-assisted reduction enabled the recovery of hydrophobicity, which coupled with the presence of a large pore volume, allowed an excellent oil absorption capacity ranging from 84 to 145 g $g^{-1}$ to be obtained. Obviously, these porous 3D structures with high surface area hold great potential for other applications, such as energy and gas storage, catalysis, and many others.

## Conflicts of interest

There are no conflicts to declare.

## Acknowledgements

All authors thank Universiti Putra Malaysia for the research facilities. Special thanks are extended to NanoMalaysia Berhad and Tex Cycle Technology (M) Berhad for the funding of this project. The findings and observations contained in this paper are those of the authors and do not necessarily reflect the funders' views. Nurul Aqilah Pohan would like to thank the Ministry of Higher Education Malaysia for the Special Graduate Research Allowance Scheme through the Fundamental Research Grant Scheme (FRGS) 5540120.

## References

1 BP, *BP Statistical Review of World Energy 2020*, London: BP Statistical Review of World Energy, available at https://www.bp.com/en/global/corporate/energy-economics/statistical-review-of-world-energy.html, accessed 18 August 2020, 2015.
2 BBC News, *Why the Mauritius oil spill is so serious*, retrieved from https://www.bbc.com/news/world-africa-53754751, accessed 8 August 2020, 2020.
3 S. Gupta and N.-H. Tai, Carbon materials as oil sorbents: a review on the synthesis and performance, *J. Mater. Chem. A.*, 2016, **4**, 1550.
4 S. Kulandaivalu and Y. Sulaiman, Designing an advanced electrode of mixed carbon materials layered on polypyrrole/reduced graphene oxide for high specific energy supercapacitor, *J. Power Sources*, 2019, **419**, 181–191.
5 F. M. Fartas, J. Abdullah, N. A. Yusof, Y. Sulaiman and M. I. Saiman, Biosensor based on tyrosinase immobilized on graphene-decorated gold nanoparticle/chitosan for phenolic detection in aqueous, *Sensors*, 2017, **17**(5), 1132.
6 T. C. Dos Santos and C. M. Ronconi, Self-assembled 3D mesoporous graphene oxides (MEGOs) as adsorbents and recyclable solids for $CO_2$ and $CH_4$ capture, *J. CO2 Util.*, 2017, **20**(June), 292–300.

7 H. Qiu, Y. Guan, P. Luo and Y. Wang, Biosensors and Bioelectronics Recent advance in fabricating monolithic 3D porous graphene and their applications in biosensing and biofuel cells, *Biosens. Bioelectron.*, 2017, **89**, 85–95.
8 B. F. Machado and P. Serp, Graphene-based materials for catalysis, *Catal. Sci. Technol.*, 2012, **2**(1), 54–75.
9 M. R. Gandhi, S. Vasudevan, A. Shibayama and M. Yamada, Graphene and Graphene-Based Composites: A Rising Star in Water Purification - A Comprehensive Overview, *ChemistrySelect*, 2016, **1**(15), 4358–4385.
10 K. S. Novoselov and A. K. Geim, Electric field effect in atomically thin carbon films, *Science*, 2004, **306**, 666–669.
11 A. Gupta, T. Sakthivel and S. Seal, Recent development in 2D materials beyond graphene, *Prog. Mater. Sci.*, 2015, **73**, 44–126.
12 B. Y. Z. Hiew, L. Y. Lee, X. J. Lee, S. Thangalazhy-Gopakumar, S. Gan, S. S. Lim and P. S. Khiew, Review on synthesis of 3D graphene-based configurations and their adsorption performance for hazardous water pollutants, *Process Saf. Environ. Prot.*, 2018, **116**, 262–286.
13 S. Nardecchia, D. Carriazo, M. L. Ferrer, M. C. Gutiérrez and F. del Monte, Three dimensional macroporous architectures and aerogels built of carbon nanotubes and/or graphene: Synthesis and applications, *Chem. Soc. Rev.*, 2013, **42**, 794–830.
14 U. M. Patil, R. V. Ghorpade, M. S. Nam, A. C. Nalawade, S. Lee, H. Han and S. C. Jun, PolyHIPE derived freestanding 3D carbon foam for cobalt hydroxide nanorods based high performance supercapacitor, *Sci. Rep.*, 2016, **6**, 35490.
15 Y. He, J. Li, K. Luo, L. Li, J. Chen and J. Li, Engineering reduced graphene oxide aerogel produced by effective γ-ray radiation-induced self-assembly and its application for continuous oil–water separation, *Ind. Eng. Chem. Res.*, 2016, **55**(13), 3775–3781.
16 X. F. Jiang, X. B. Wang, P. Dai, X. Li, Q. Weng, X. Wang and D. Golberg, High-throughput fabrication of strutted graphene by ammonium-assisted chemical blowing for high-performance supercapacitors, *Nano Energy*, 2015, **16**, 81–90.
17 H. Bai, C. Li and G. Shi, A pH-sensitive graphene oxide composite hydrogel, *Chem. Commun.*, 2010, **46**, 2376–2378.
18 X. Chen, P. K. Eggers, A. D. Slattery, S. G. Ogden and C. L. Raston, Template-free assembly of three-dimensional networks of graphene hollow spheres at the water/toluene interface, *J. Colloid Interface Sci.*, 2014, **430**, 174–177.
19 L. Ee, S. P. Siva, Y. Kuen, E. Seng and T. Tey, Recent advances of characterization techniques for the formation, physical properties and stability of Pickering emulsion, *Adv. Colloid Interface Sci.*, 2020, **277**, 102117.
20 R. Kamaraj, A. Pandiarajan, M. R. Gandhi, A. Shibayama and S. Vasudevan, Eco–friendly and Easily Prepared GrapheneNanosheets for Safe Drinking Water: Removal of Chlorophenoxyacetic Acid Herbicides, *ChemistrySelect*, 2017, **2**(1), 342–355.
21 P. Ganesan, R. Kamaraj and S. Vasudevan, Application of isotherm, kinetic and thermodynamic models for the adsorption of nitrate ions on graphene from aqueous solution, *J. Taiwan Inst. Chem. Eng.*, 2013, **44**(5), 808–814.
22 S. Vasudevan and J. Lakshmi, The adsorption of phosphate by graphene from aqueous solution, *RSC Adv.*, 2012, **2**(12), 5234–5242.
23 T. A. Tabish, F. A. Memon, D. E. Gome, D. W. Horsell and S. Zhang, A facile synthesis of porous graphene for efficient water and wastewater treatment, *Sci. Rep.*, 2018, **8**, 1817.
24 Y. Cheng, P. Xu, W. Zeng, C. Ling, S. Zhao, K. Liao and A. Zhou, Highly hydrophobic and ultralight graphene aerogel as high efficiency oil absorbent material, *J. Environ. Chem. Eng.*, 2017, **5**(2), 1957–1963.
25 H. Bi, X. Xie, K. Yin, Y. Zhou, S. Wan and L. Sun, Highly enhanced performance of spongy graphene as an oil sorbent, *J. Mater. Chem. A*, 2014, **2**, 1652.
26 S. Song, H. Yang, C. Su, Z. Jiang and Z. Lu, Ultrasonic microwave assisted synthesis of stable reduced graphene oxide modified melamine foam with superhydrophobicity and high oil adsorption capacities, *Chem. Eng. J.*, 2016, **306**, 504–511.
27 I. Sengupta, S. Chakraborty, M. Talukdar, S. K. Pal and S. Chakraborty, Thermal reduction of graphene oxide: How temperature influences purity, *J. Mater. Res.*, 2018, **33**(23), 4113–4122.
28 M. A. Riaz, P. Hadi, I. H. Abidi, A. Tyagi, X. Ou and Z. Luo, Recyclable 3D graphene aerogel with bimodal pore structure for ultrafast and selective oil sorption from water, *RSC Adv.*, 2017, **7**, 29722–29731.
29 G. Tao, L. Zhang, Z. Hua, Y. Chen, L. Guo, J. Zhang and J. Shi, Highly efficient adsorbents based on hierarchically macro/mesoporous carbon monoliths with strong hydrophobicity, *Carbon*, 2014, **66**, 547–559.
30 M. Thommes, K. Kaneko, A. V. Neimark, J. P. Olivier, F. Rodriguez-reinoso, J. Rouquerol and K. S. W. Sing, Physisorption of gases, with special reference to the evaluation of surface area and pore size distribution (IUPAC Technical Report), *Pure Appl. Chem.*, 2015, **87**(9–10), 1051–1069.
31 J.-Y. Hong, E.-H. Sohn, S. Park and H. S. Park, Highly-efficient and recyclable oil absorbing performance of functionalized graphene aerogel, *Chem. Eng. J.*, 2015, **269**, 229–235.
32 M. M. Gudarzi and F. Sharif, Self-assembly of graphene oxide at the liquid-liquid interface: A new route to the fabrication of graphene-based composites, *Soft Matter*, 2011, **7**(7), 3432–3440.
33 H. M. Afzal, F. Shehzad, M. Zubair, O. Y. Bakather and M. A. Al-Harthi, Influence of microwave irradiation on thermal properties of PVA and PVA/graphene nanocomposites, *J. Therm. Anal. Calorim.*, 2020, **139**(1), 353–365.
34 Y. He, Y. Liu, T. Wu, J. Ma, X. Wang, Q. Gong and J. Gao, An environmentally friendly method for the fabrication of reduced graphene oxide foam with a super oil absorption capacity, *J. Hazard. Mater.*, 2013, **260**, 796–805.

35 D. D. Nguyen., T. Nyan-Hwa, L. San-Boh and W.-S. Kuob, Superhydrophobic and superoleophilic properties of graphene-based sponges fabricated using a facile dip coating method, *Energy Environ. Sci.*, 2012, **5**, 7908–7912.

36 Y. Liu, J. Ma, T. Wu, X. Wang, G. Huang, Y. Liu and J. Gao, Cost-effective reduced graphene oxide-coated polyurethane sponge as a highly efficient and reusable oil-absorbent, *ACS Appl. Mater. Interfaces*, 2013, **5**(20), 10018–10026.

37 J. T. Korhonen, M. Kettunen, R. H. Ras and O. Ikkala, Hydrophobic nanocellulose aerogels as floating, sustainable, reusable, and recyclable oil absorbents, *ACS Appl. Mater. Interfaces*, 2011, **3**(6), 1813–1816.

38 S. J. Yang, J. H. Kang, H. Jung, T. Kim and C. R. Park, Preparation of a freestanding, macroporous reduced graphene oxide film as an efficient and recyclable sorbent for oils and organic solvents, *J. Mater. Chem. A.*, 2013, **1**(33), 9427–9432.

39 Y. Chu and Q. Pan, Three-dimensionally macroporous Fe/C nanocomposites as highly selective oil-absorption materials, *ACS Appl. Mater. Interfaces*, 2012, **4**(5), 2420–2425.

40 H. Bi, X. Huang, X. Wu, X. Cao, C. Tan, Z. Yin and H. Zhang, Carbon microbelt aerogel prepared by waste paper: an efficient and recyclable sorbent for oils and organic solvents, *Small*, 2014, **10**(17), 3544–3550.

41 H. Bi, Z. Yin, X. Cao, X. Xie, C. Tan, X. Huang and X. Lu, Carbon fiber aerogel made from raw cotton: a novel, efficient and recyclable sorbent for oils and organic solvents, *Adv. Mater.*, 2013, **25**(41), 5916–5921.

42 S. Huang and J. Shi, Monolithic macroporous carbon materials as high-performance and ultralow-cost sorbents for efficiently solving organic pollution, *Ind. Eng. Chem. Res.*, 2014, **53**(12), 4888–4893.

43 Y. Zhao, C. Hu, Y. Hu, H. Cheng, G. Shi and L. Qu, A versatile, ultralight, nitrogen-doped graphene framework, *Angew. Chem., Int. Ed.*, 2012, **51**(45), 11371–11375.

44 Z. Niu, J. Chen, H. H. Hng, J. Ma and X. Chen, A Leavening Strategy to Prepare Reduced Graphene Oxide Foams, *Adv. Mater.*, 2012, **24**, 4144–4150.

45 B. Li, X. Liu, X. Zhang, J. Zou, W. Chai and J. Xu, Oil-absorbent polyurethane sponge coated with KH-570-modified graphene, *J. Appl. Polym. Sci.*, 2015, **41821**, 1–7.

46 S. Zhou, G. Hao, X. Zhou, W. Jiang, T. Wang, N. Zhang and L. Yu, One-pot synthesis of robust superhydrophobic, functionalized graphene/polyurethane sponge for effective continuous oil – water separation, *Chem. Eng. J.*, 2016, **302**, 155–162.

47 J. Peng, J. Deng, Y. Quan, C. Yu, H. Wang, Y. Gong and W. Deng, Superhydrophobic Melamine Sponge Coated with Striped Polydimethylsiloxane by Thiol–Ene Click Reaction for Efficient Oil/Water Separation, *ACS Omega*, 2018, **3**, 5222–5228.

48 W. Wenchao, R. Zhang., Li. Wei, H. Liu., Y. Lin., L. Li. and Y. Zhou., Graphene–carbon nanotube aerogel as an ultralight, compressible and recyclable highly efficient absorbent for oil and dyes, *Environ. Sci.: Nano*, 2016, **3**, 107–113.

49 N. A. Ibrahim, C. B. Woei and M. Z. Hussein, *Method of Producing a Dispersible Nano Graphene or Graphene Oxide*, Patent Application No: PI2014700668, 2014.

50 D. C. Marcano, D. V. Kosynkin, J. M. Berlin, A. Sinitskii, Z. Sun, A. S. Slesarev and J. M. Tour, Correction to Improved Synthesis of Graphene Oxide, *ACS Nano*, 2018, **12**(2), 2078.

51 B. J. Liang, Y. Huang, L. Zhang, Y. Wang, Y. Ma, T. Guo and Y. Chen, Molecular-Level Dispersion of Graphene into Polyvinyl alcohol and Effective Reinforcement of their Nanocomposites, *Adv. Funct. Mater.*, 2009, **19**, 2297–2302.

52 W. Chen, L. Yan and P. R. Bangal, Preparation of graphene by the rapid and mild thermal reduction of graphene oxide induced by microwaves, *Carbon*, 2010, **48**(4), 1146–1152.